ASTRONOMY

Direct detection of an asteroid's heliocentric deflection: The Didymos system after DART

Rahil Makadia[1]*†, Steven R. Chesley[2]†, David Herald[3], Davide Farnocchia[2], Nancy L. Chabot[4], Shantanu P. Naidu[2], Andrew S. Rivkin[4], Alexandros Siakas[5], Damya Souami[6,7,8], Paolo Tanga[7], Sotirios Tsavdaridis[5], Kleomenis Tsiganis[5], Sébastien Bouquillon[9], Siegfried Eggl[1]

In September 2022, NASA's Double Asteroid Redirection Test (DART) spacecraft crashed into Dimorphos and demonstrated the kinetic impact method of protecting Earth from asteroids. A fraction of the impulse delivered to Dimorphos was also imparted onto the Didymos system's barycenter, changing its heliocentric orbit. Here, we present the first-ever measurement of human-caused change in the heliocentric orbit of a celestial body. Thanks to stellar occultation and radar measurements, we estimate that the Didymos system experienced an along-track velocity change of −11.7 ± 1.3 micrometers per second. We constrain the heliocentric momentum enhancement factor for DART at 2.0 ± 0.3 and the bulk densities of Didymos and Dimorphos at 2600 ± 140 and 1540 ± 220 kilograms per cubic meter, respectively. Our results demonstrate that targeting the secondary asteroid in binary systems constitutes a possible strategy for kinetic impact deflection, adding to humanity's planetary defense capabilities.

INTRODUCTION

Earth is hit by tens of tons of dust and small particles every day (*1*). Furthermore, small asteroids less than 5 m in diameter affect the Earth every year (*2*). On a much less frequent but certainly nonnegligible basis, the Earth has been hit by larger asteroids (*3*–*4*). Fortunately, asteroid impacts can be avoided with current technology if three primary goals are accomplished.

First, asteroids large enough to survive entry into our atmosphere need to be detected and cataloged. This is a nontrivial process, and most Near-Earth Objects (NEOs) larger than 140 m remain unfound (*5*). However, both existing and upcoming surveys are slated to markedly increase detection rates for NEOs, some of which could be Earth impactors (*6*–*10*). Second, we need to assess the Earth impact hazard for each newly discovered NEO. If provided sufficient observation data, then current impact monitoring capabilities of the Center for Near-Earth Objects at NASA's Jet Propulsion Laboratory (JPL) and the European Space Agency's Near-Earth Objects Coordination Centre can accurately assess the impact hazard of NEOs (*11*–*12*). Third, we need to develop efficient and effective strategies to change the orbit of incoming asteroids. This is another nontrivial challenge, but it is one we now have at least some experience with.

On 26 September 2022, NASA's Double Asteroid Redirection Test (DART) spacecraft intentionally affected Dimorphos, the moon of asteroid (65803) Didymos (*13*). The impact successfully completed the mission's primary objective of demonstrating the kinetic impact technique as a viable method of deflecting asteroids. As a result, Dimorphos now orbits Didymos with a period 33 min shorter than before the DART impact (*14*–*16*).

A key property of the kinetic impact deflection method is that after the impact, material from the target asteroid's surface is launched into space, creating a plume of ejecta (*17*). This ejecta plume can be observed (*18*–*19*), and the momentum carried away from the target asteroid by the ejecta adds to the momentum imparted by the kinetic impactor. The ratio of the total momentum imparted by the impact event (i.e., impactor spacecraft plus ejecta) to the momentum imparted by the spacecraft alone is known as the momentum enhancement factor, β. Here, we use the scalar interpretation of β and project it in various directions of interest (*20*). Each value of the momentum enhancement factor here is accompanied by a subscript that clarifies that β is a directional quantity. For example, the along-track momentum enhancement factor (which is projected along the linear momentum of the target, $\vec{p}$) is written as β_p.

Another consequence of the DART impact on Dimorphos was that some amount of ejecta escaped the Didymos-Dimorphos system (*18*–*19*). As a result of the momentum imparted by the DART spacecraft and this system-escaping ejecta, the system's barycenter was also deflected, causing a change in the heliocentric orbit. Therefore, there are two types of different momentum enhancement factors that need to be considered. The first is the mutual orbit along-track momentum enhancement factor to characterize the ejecta that contributed to the change in the orbital period of Dimorphos, $\beta_{p,\mathrm{dim}}$. For an assumed Dimorphos bulk density of 2400 kg m^{-3}, this along-track momentum enhancement factor has been calculated to be $\beta_{p,\mathrm{dim}} = 3.61^{+0.19}_{-0.25}$ in previous work (*21*). However, that estimate assumed perfect knowledge of Dimorphos's bulk density. The same study reported an estimate of $\beta_{p,\mathrm{dim}}$ falling between 2.2 and 4.9 when assuming a plausible range of densities.

The second flavor of β is the heliocentric momentum enhancement factor, $\beta_\odot$, which is parametrized by the ejecta momentum that escapes the gravitational influence of the entire binary asteroid system. When projected in the system's along-track direction, it can be written as $\beta_{p,\odot}$. This value is of special interest from a planetary defense perspective because it provides information about changes

[1]University of Illinois Urbana-Champaign, Urbana, IL 61801, USA. [2]Jet Propulsion Laboratory, California Institute of Technology, Pasadena, CA 91109, USA. [3]Trans Tasman Occultation Alliance & International Occultation Timing Association, Wellington 6011, New Zealand. [4]Johns Hopkins University Applied Physics Laboratory, Laurel, MD 20723, USA. [5]Aristotle University of Thessaloniki, Thessaloniki 54124, Greece. [6]LIRA, CNRS UMR8254, Observatoire de Paris - PSL, Sorbonne Univ., Univ. Paris Cité, CY Cergy Paris Univ., Meudon, 92190, France. [7]Laboratoire Lagrange, Université Côte d'Azur, Observatoire de la Côte d'Azur, CNRS, Nice 06300, France. [8]naXys, Department of Mathematics, University of Namur, Namur 5000, Belgium. [9]LTE, Observatoire de Paris, Université PSL, CNRS, Sorbonne Université, Paris 75014, France.
*Corresponding author. Email: makadia2@illinois.edu
†These authors contributed equally to this work.

in the system's trajectory about the sun, in particular the orbital period, which would be the most relevant quantity in an actual asteroid impact scenario. Before DART impact, a statistical exploration of the possible values of $\beta_\odot$ showed that there was no practical possibility that the Didymos system would be put on a collision course with the Earth as a result of DART (*22*). After the DART impact, focus shifted to the measurability of $\beta_\odot$ (*23*). This initial postimpact effort showed that $\beta_\odot$ should be measurable using ground-based stellar occultation measurements in the second half of 2024 because they can provide milliarcsecond-level astrometry of asteroids (*24*). However, the actual value of $\beta_\odot$ for DART has not been determined to date.

RESULTS AND DISCUSSION

We now have 22 stellar occultation measurements of Didymos between October 2022 and March 2025. Thanks to the longer observation arc provided by the last four of these observations between May 2024 and March 2025, we can now estimate the heliocentric deflection of the entire binary asteroid system caused by the DART spacecraft. As of 1 May 2025, the observational data for Didymos consist of 5955 ground-based right ascension and declination pairs, 22 stellar occultation measurements, 3 optical navigation measurements from the DART spacecraft during approach, and 9 ground-based radar delay measurements.

We pursued two avenues to estimate the value of $\beta_\odot$ using the observations. The first entailed directly estimating the value of $\beta_\odot$ for a given system-escaping ejecta momentum vector (*23*). The second method, which is used in this work, allowed us to estimate the full heliocentric velocity change vector, $\Delta\vec{V}_\odot$. We then projected this vector in the along-track direction and computed the value of $\beta_{p,\odot}$ using momentum conservation laws. More details on this approach can be found in Materials and Methods. Both methods were implemented in the Gauss-Radau Small-body Simulator library (*25*). They provided consistent estimates of $\beta_\odot$, differing only at a level of 0.01σ.

Furthermore, the value of $\Delta\vec{V}_\odot$ projected in the along-track direction to provide $\Delta V_{p,\odot}$ was also estimated using an independent software library (JPL's Comet and Asteroid Orbit Determination Programs). Both software suites provided statistically consistent values, differing only at the 0.1σ level. These tests served as validation of the tools and mathematical models used in this work.

We then connected the heliocentric and mutual orbit changes as a result of DART using $\Delta V_{p,\odot}$ and κ_p, which is the fraction of along-track ejecta momentum that escaped the system as opposed to only escaping Dimorphos's gravitational influence. More details on how this is done can be found in Materials and Methods. Using this connection, we computed the along-track momentum enhancement factor for the mutual orbit ($\beta_{p,\mathrm{dim}}$) and the mass of Dimorphos (m_{dim}). This, in turn, enabled the calculation of the densities of Didymos (ρ_{didy}) and Dimorphos (ρ_{dim}). The corresponding values are reported in Table 1.

The $\Delta V_{p,\odot}$ detection is significant at almost 9σ, and $\beta_{p,\odot}$ is significant at nearly 7σ. Therefore, these estimates are not ambiguous in a statistical sense. The value of $\beta_{p,\odot} \simeq 2$ implies that the spacecraft and system-escaping ejecta imparted roughly equal along-track deflections to the system. The estimated value of $\beta_{p,\mathrm{dim}}$ is lower than the previously reported nominal value (*21*) of $\beta_{p,\mathrm{dim}} = 3.61^{+0.19}_{-0.25}$. That estimate assumed a perfectly known density of 2400 kg m^{-3} for Dimorphos, which is more than 3σ away from the estimated Dimorphos density from this work. When the density from this work (and its associated uncertainty) is consistently folded into the $\beta_{p,\mathrm{dim}}$ scaling relationship provided by previous results (*21*), the two estimates are statistically consistent at the 0.6σ level.

Our results reveal that both the mass (m_{dim}) and density (ρ_{dim}) of Dimorphos are lower than those presented in previous studies (*21*, *26*). However, recent work on forward modeling of the DART impact has already suggested that Dimorphos is substantially underdense with respect to Didymos (*27*). Furthermore, spectroscopy of the Didymos system shows that it belongs to the S-type asteroid class (*28*). Figure 1 shows the densities of Didymos and Dimorphos compared to other S-type single and binary asteroids. This plot shows that the densities estimated in this work are consistent with previous ground- and space-based density measurements of S-type asteroids. The density of Didymos (ρ_{didy}) estimated here falls within the range of typical densities of S-type asteroids (*29*). Although Dimorphos's density is rather lower, it is still in family with the densities of (25143) Itokawa (*30*–*31*) and (66391) Moshup (*32*). The low density for Dimorphos would also be a natural result of the prevailing theory that Dimorphos formed via accretion of mass that was

Table 1. Summary of the parameters estimated in this work. The nominal values and their corresponding 1σ uncertainties are reported.

Parameter	Value ± Uncert. (1σ)
$\Delta V_{p,\odot}$ [μm s^{-1}]	−11.7 ± 1.3
$\beta_{p,\odot}$	2.0 ± 0.3
$\beta_{p,\mathrm{dim}}$	2.1 ± 0.3
m_{dim} [10^9 kg]	2.7 ± 0.4
ρ_{dim} [kg m^{-3}]	1540 ± 220
ρ_{didy} [kg m^{-3}]	2600 ± 140
m_{dim} / m_{didy}	0.0051 ± 0.0006
$\beta_{\mathrm{n,dim}}$	1.9 ± 0.3

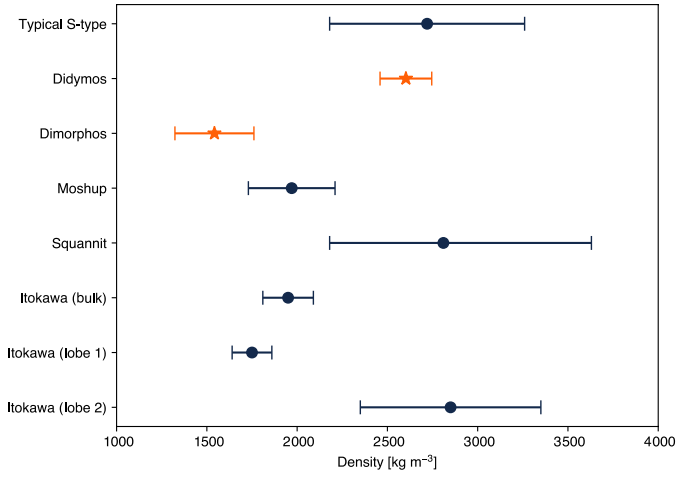

Fig. 1. Densities (and corresponding 1σ uncertainties) of S-type asteroids. The orange starred error bars show the density estimates from this work. The blue dotted error bars are from previous estimates (*29*–*32*).

shed by an accelerating rotation of Didymos (*33*–*35*). By combining the density and volume estimates of the two asteroids, we also compute the mass ratio ($m_{\mathrm{dim}} / m_{\mathrm{didy}}$) of the Didymos system in Table 1. This result implies that Didymos is almost 200 times more massive than Dimorphos, which is also in line with known information about multi-asteroid systems (*36*). As expected, the magnitude of the barycenter deflection ($\simeq -13\ \mu\mathrm{m\ s}^{-1}$; see table S1) is smaller than the Dimorphos deflection ($\simeq -2600\ \mu\mathrm{m\ s}^{-1}$) (*15*) by a factor close to the mass ratio.

Figure 2 shows the estimated values of $\beta_{p,\odot}$ and ρ_{dim} as a function of the direction in which ejecta momentum escaped from the binary asteroid system. The error bar represents the nominal value and uncertainties for the direction of the ejecta momentum vector based on previous work (*37*). These results show that in light of their respective uncertainties, the values of $\beta_{p,\odot}$ and ρ_{dim} are relatively insensitive to the chosen direction of the escaping ejecta momentum vector. This means that the estimates presented here are robust to differences in the direction in which the ejecta escaped the Didymos system compared to the direction of Dimorphos-escaping ejecta. Furthermore, after the system mass uncertainty (which is an epistemic uncertainty and can therefore still be refined with new measurements), uncertainty in the ejecta direction is the largest contributor to the $\Delta V_{p,\odot}$ uncertainty. Understanding the contribution of this uncertainty helps establish a floor on the achievable accuracy of future $\beta_{p,\odot}$ estimates.

Another useful quantity that facilitates the extension of DART results to future kinetic impactor missions is the surface normal momentum enhancement factor, β_{n}. In contrast to β_p, β_{n} projects the deflection along the surface normal vector of the asteroid at the impact site. Because surface normal vectors for potential kinetic impact sites can be obtained from shape models of asteroids, projecting the DART-Dimorphos momentum exchange along this direction can help predict the outcomes of future asteroid deflection missions. For the DART mission, we find that $\beta_{\mathrm{n,dim}} = 1.9 \pm 0.3$. However, we note that the DART spacecraft affected Dimorphos in between boulders (*38*). Therefore, the surface normal direction of the impact site is not well defined. For this reason, we suggest inflating the uncertainty in $\beta_{\mathrm{n,dim}}$ for future use in modeling kinetic impact deflections.

This work adds the capability of deflecting a binary asteroid system in its heliocentric orbit to the list of novel technologies demonstrated by the DART mission (*13*). As expected, the measured impulse on the Didymos system as a result of DART is smaller than the change in Dimorphos's orbit around Didymos because the heliocentric deflection as a result of affecting Dimorphos is proportional to the system mass ratio. We highlight that the estimated value for $\beta_{\odot}$ is well within the range considered in previous work (*22*) and that the Earth remains safe from the Didymos system for at least the next 100 years. Further refinements can be made to our results once the European Space Agency's Hera spacecraft (*39*) arrives at the Didymos system. Using Hera navigation data, geocentric pseudorange measurements can be generated for the Didymos system barycenter as was done for the OSIRIS-REx spacecraft at Bennu (*40*). These measurements can then be added to the existing astrometric data to refine the estimates presented here. By demonstrating that asteroid deflection missions such as DART can effect change in the heliocentric orbit of a celestial body, this study marks a notable step forward in our ability to prevent future asteroid impacts on Earth.

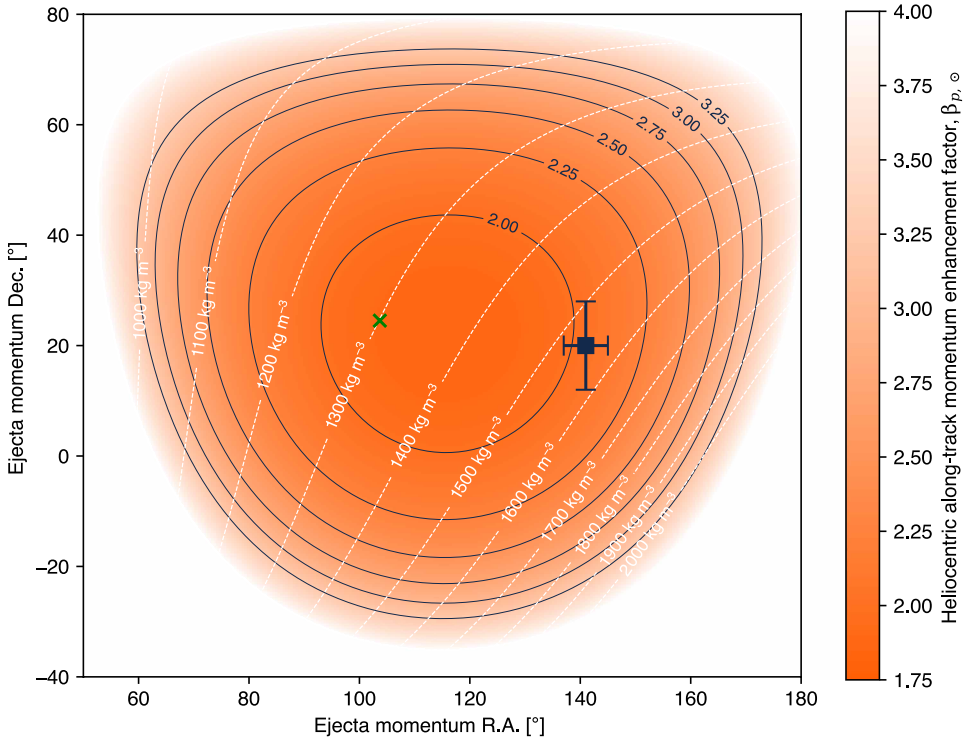

Fig. 2. $\beta_{p,\odot}$ and ρ_{dim} as a function of different system-escaping ejecta momentum directions defined using right ascension and declination. The solid contours and the color bar represent the values of $\beta_{p,\odot}$, and the dashed contours show the values of ρ_{dim}. The error bars represent the nominal value (and the corresponding 1σ uncertainty) of the Dimorphos-escaping ejecta momentum direction (*37*). The cross marks the Didymos system along-track direction. R.A., right ascension; Dec., declination.

MATERIALS AND METHODS

Joint orbit determination and $\Delta\vec{V}_{\odot}$ estimation

The primary method of estimating the quantities measured in this work is orbit determination using a nonlinear weighted least squares filter (*25*, *41*). As mentioned in Results and Discussion, the dataset for Didymos consists of nearly 6000 observations over 29 years and is obtained from publicly available information at the Minor Planet Center. To make sure spurious observations did not affect the orbit estimate, we used an outlier rejection algorithm (*42*) with a rejection threshold of $\chi = 2$. This resulted in the rejection of two stellar occultation observations and 72 ground-based astrometric measurements. In the case of Didymos, the filter is used to estimate not just the orbital elements and the A_2 transverse nongravitational acceleration parameter for the Yarkovsky effect (*43*) but also the change in velocity ($\Delta\vec{V}_{\odot}$) vector for the Didymos system barycenter at the moment of the DART impact. A similar formulation was previously used to search for collisions of near-Earth asteroid (3908) Nyx with main-belt asteroids (*44*). The estimated orbit solution is presented in table S1. The residuals for the occultation observations used in the orbit solution are presented in table S2.

By estimating the $\Delta\vec{V}_{\odot}$ vector and obtaining a corresponding covariance matrix, we did not project the momentum exchange along any direction and made no forced assumptions about the direction in which the ejecta escaped during the orbit fitting process. To aid filter convergence, we applied a priori constraints on the three components of the $\Delta\vec{V}_{\odot}$ vector (*45*). The prior estimate and its corresponding covariance for $\Delta\vec{V}_{\odot}$ were based on the model for the change in velocity of a target asteroid due to a kinetic impact (*46*), which is written as

$$\Delta\vec{V}_{\odot} = \frac{m_{\mathrm{DART}}}{m_{\mathrm{sys}}}\left[\vec{V}_{\infty} + \left(\beta_{\odot} - 1\right)\left(\vec{V}_{\infty}\cdot\hat{e}_{*}\right)\hat{e}_{*}\right] \quad (1)$$

Here, $\Delta\vec{V}_{\odot}$ is the heliocentric change in velocity of the binary system, m_{sys} is the total mass of the binary system, $m_{\mathrm{DART}} \ll m_{\mathrm{sys}}$ is the mass of the DART spacecraft at impact, $\vec{V}_{\infty}$ is the relative velocity of the DART spacecraft with respect to the binary system at impact, $\beta_{\odot}$ is the heliocentric momentum enhancement factor, and $\hat{e}_{*}$ is the escaping ejecta momentum direction. When we began this work, no information was available for $\beta_{\odot}$. Therefore, we assumed that $\beta_{\odot}$ was uniformly distributed in the range [1, 5] to remain consistent with a broad range of existing predictions (*47*), which were eventually confirmed by our results. We convolved this uniform distribution with known values of other variables in Eq. 1, which are listed in table S5. We then computed the a priori distribution (mean and covariance) for $\Delta\vec{V}_{\odot}$ by drawing 1 million samples from each contributing variable. The resulting a priori constraints, shown in table S3, were used to estimate the results presented in Table 1.

To make sure that the a priori constraints did not bias the final estimate, we repeated the estimation process twice: once with the prior covariance multiplied by a factor of 2 and another time with the prior covariance matrix divided by 2. Doing so negligibly altered the uncertainties in $\Delta V_{p,\odot}$ by 2.5%. In addition, these changes to the prior covariance only shifted the nominal estimate of $\Delta V_{p,\odot}$ at a statistically insignificant level of 0.2σ.

Next, we repeated the same test by halving or doubling the prior value of $\Delta\vec{V}_{\odot}$. Doing so shifted the nominal estimate of $\Delta V_{p,\odot}$ by 0.7σ. The larger change when altering the prior mean is expected because we were directly forcing the solution to unrealistically small or large values. The fact that the shift is small demonstrates the robustness of the nominal estimate. Therefore, the computed priors did not have any unintended effects on the orbit solution.

Successful convergence of the filter using this method yielded a $\Delta\vec{V}_{\odot}$ vector and a corresponding 3 by 3 covariance matrix. Once we had this information, we could project the $\Delta\vec{V}_{\odot}$ along any direction of interest. In the context of planetary defense, it is more intuitive and useful to project this deflection in the system heliocentric along-track direction (*20*), $\hat{e}_{p,\odot}$, which yields an estimate of $\Delta V_{p,\odot} = \Delta\vec{V}_{\odot}\cdot\hat{e}_{p,\odot} = -11.7 \pm 1.3\,\mu\mathrm{m\,s^{-1}}$. This is the value reported in Table 1. This heliocentric velocity change corresponds to a -360 ± 40 m change in the semimajor axis of the system's orbit around the Sun, which corresponds to a 150 ± 20 ms reduction in the system's 2.1-year orbital period.

Computing the momentum enhancement factors and densities from $\Delta V_{p,\odot}$

We started by projecting Eq. 1 into the heliocentric along-track direction of the Didymos system, $\hat{e}_{p,\odot}$. This direction is in line with the velocity vector of the binary system barycenter ($\hat{V}_{\odot}\cdot\hat{e}_{p,\odot} = 1$)

$$\Delta\vec{V}_{\odot}\cdot\hat{e}_{p,\odot} = \Delta V_{p,\odot} = \frac{m_{\mathrm{DART}}}{m_{\mathrm{sys}}}\left[\vec{V}_{\infty} + \left(\beta_{p,\odot} - 1\right)\left(\vec{V}_{\infty}\cdot\hat{e}_{*}\right)\hat{e}_{*}\right]\cdot\hat{e}_{p,\odot} \quad (2)$$

which, after some algebraic manipulation, becomes

$$\frac{m_{\mathrm{sys}}}{m_{\mathrm{DART}}}\Delta V_{p,\odot} = \vec{V}_{\infty}\cdot\hat{e}_{p,\odot} + \left(\beta_{p,\odot} - 1\right)\left(\vec{V}_{\infty}\cdot\hat{e}_{*}\right)\hat{e}_{*}\cdot\hat{e}_{p,\odot} \quad (3)$$

Here, $\Delta V_{p,\odot}$ is the along-track component of the heliocentric change in velocity of the binary system ($\Delta\vec{V}_{\odot}$), and $\beta_{p,\odot}$ is the heliocentric along-track momentum enhancement factor. Rearranging the equation for $\beta_{p,\odot}$, we have

$$\beta_{p,\odot} = 1 + \frac{m_{\mathrm{sys}}\Delta V_{p,\odot} - m_{\mathrm{DART}}\vec{V}_{\infty}\cdot\hat{e}_{p,\odot}}{m_{\mathrm{DART}}\left[\left(\vec{V}_{\infty}\cdot\hat{e}_{*}\right)\hat{e}_{*}\cdot\hat{e}_{p,\odot}\right]} \quad (4)$$

On the basis of Eq. 3, we wrote an analogous expression for the mutual orbit along-track velocity change ($\Delta V_{p,\mathrm{dim}}$), which corresponds to the orbit of Dimorphos around Didymos. This was done using the mutual orbit along-track momentum enhancement factor, $\beta_{p,\mathrm{dim}}$, and the mutual orbit along-track direction of Dimorphos, $\hat{e}_{p,\mathrm{dim}}$ [taken from JPL orbit solution 547 for Dimorphos (*15*)], which results in

$$\frac{m_{\mathrm{dim}}}{m_{\mathrm{DART}}}\Delta V_{p,\mathrm{dim}} = \vec{V}_{\infty}\cdot\hat{e}_{p,\mathrm{dim}} + \left(\beta_{p,\mathrm{dim}} - 1\right)\left(\vec{V}_{\infty}\cdot\hat{e}_{*}\right)\hat{e}_{*}\cdot\hat{e}_{p,\mathrm{dim}} \quad (5)$$

To relate $\beta_{p,\odot}$ and $\beta_{p,\mathrm{dim}}$, we define κ_p as the ratio of the system-escaping ejecta momentum traveling along the system's along-track direction to the ejecta momentum that escaped Dimorphos's gravity in its own along-track direction. Although the two along-track directions do not perfectly align, κ_p is still an important metric because it quantifies how much material left the system versus how much of the ejecta fell back onto Didymos or remained gravitationally bound within the system. As a result, a portion of the along-track ejecta momentum that escaped Dimorphos did not escape the binary system. κ_p is written as

$$\kappa_p = \frac{\beta_{p,\odot} - 1}{\beta_{p,\mathrm{dim}} - 1} \tag{6}$$

If no ejecta escaped the Didymos system, then $\kappa_p = 0$. This is not the case in view of the measured heliocentric along-track ΔV and the imagery showing the escaping ejecta (*18*–*19*). If more ejecta momentum escaped the system in the heliocentric system along-track direction than the momentum that escaped Dimorphos in the mutual orbit along-track direction, then $\kappa_p > 1$. This is an implausible scenario for the DART impact because the spacecraft's velocity vector, the Dimorphos along-track direction, and the system along-track direction at impact are roughly aligned. If the Dimorphos along-track direction and the system along-track direction were perfectly aligned, then $\kappa_p \in [0, 1]$. Therefore, κ_p is a proxy for the fraction of along-track ejecta momentum that escaped the system after the impact.

From previous work (*15*), we know that the instantaneous value of the change in Dimorphos's orbital period was −1961 s. However, we also know that the steady-state value of this orbit period change a few weeks after impact was −1995 s (*15*). This means that some fraction of the Dimorphos along-track ejecta momentum was temporarily trapped in the system. Escape of this trapped momentum altered the value of Dimorphos's mutual orbit period change by −34 s or 1.7% of the steady-state period change. This 1.7% value gives an order-of-magnitude estimate for the amount of ejecta momentum that remained trapped in the system. As a conservative upper bound, we assumed that 10% of the along-track momentum that escaped Dimorphos could have stayed trapped in the system ($\kappa_p \sim \mathrm{U}[0.9, 1.0]$). This led to a mean value of $\kappa_p = 0.95$ and an SD of $(1.0-0.9)/\sqrt{12} \approx 0.03$. Equation 5 could now be rewritten using κ_p and solved for m_{dim}

$$\frac{m_{\mathrm{dim}}}{m_{\mathrm{DART}}}\Delta V_{p,\mathrm{dim}} = \vec{V}_\infty \cdot \hat{e}_{p,\mathrm{dim}} + \frac{(\beta_{p,\odot} - 1)}{\kappa_p}\left(\vec{V}_\infty \cdot \hat{e}_*\right)\hat{e}_* \cdot \hat{e}_{p,\mathrm{dim}}$$

$$m_{\mathrm{dim}} = \frac{m_{\mathrm{DART}}\left[\kappa_p \vec{V}_\infty \cdot \hat{e}_{p,\mathrm{dim}} + (\beta_{p,\odot} - 1)\left(\vec{V}_\infty \cdot \hat{e}_*\right)\hat{e}_* \cdot \hat{e}_{p,\mathrm{dim}}\right]}{\kappa_p \Delta V_{p,\mathrm{dim}}} \tag{7}$$

The value of Dimorphos's mass was combined with its volume (*26*) ($\mathbb{V}_{\mathrm{dim}}$) to compute Dimorphos's bulk density, $\rho_{\mathrm{dim}} = m_{\mathrm{dim}} / \mathbb{V}_{\mathrm{dim}}$. Although κ_p is necessary to connect the mutual orbit changes, the nominal estimates in this work are not particularly sensitive to the value of κ_p. Table S4 shows the effects of varying κ_p on the estimated quantities. Expanding the range to an unrealistic value of $\kappa_p = [0.25, 1.0]$ only alters the estimated parameters by about 1σ. This is because the uncertainty of the other input parameters in Eq. 7 is larger than the contributions of the uncertainty in κ_p. If the Dimorphos density is larger than reported in Table 1, this would indicate that more ejecta were initially trapped in the system. Conversely, if we obtain an independent Dimorphos density estimate from the Hera mission (*39*) when it arrives at the system, then we can independently estimate κ_p.

Because estimates for the system mass and Didymos volume ($\mathbb{V}_{\mathrm{didy}}$) were also provided in previous work (*15*, *34*), we computed the Didymos density as

$$\rho_{\mathrm{didy}} = \frac{(m_{\mathrm{sys}} - m_{\mathrm{dim}})}{\mathbb{V}_{\mathrm{didy}}} \tag{8}$$

Previous work (*15*) estimated the radial and along-track components of the change in Dimorphos's velocity due to the DART impact. Given that Dimorphos's pre-DART orbit has been assumed circular (*15*), we combined the radial, along-track, and angular momentum directions to form an orthonormal basis. The radial direction ($\hat{e}_{\mathrm{r,dim}}$) points from Didymos to Dimorphos. The along-track direction ($\hat{e}_{p,\mathrm{dim}}$) is in line with Dimorphos's velocity about Didymos, and the angular momentum direction ($\hat{e}_{h,\mathrm{dim}}$) is defined by their cross product. Using the estimates of the change in Dimorphos's velocity in these three directions, we calculated the full Dimorphos change in velocity vector, $\Delta\vec{V}_{\mathrm{dim}}$, as

$$\Delta\vec{V}_{\mathrm{dim}} = \Delta V_{\mathrm{r,dim}}\hat{e}_{\mathrm{r,dim}} + \Delta V_{p,\mathrm{dim}}\hat{e}_{p,\mathrm{dim}} + \Delta V_{h,\mathrm{dim}}\hat{e}_{h,\mathrm{dim}} \tag{9}$$

Here, $\Delta V_{\mathrm{r,dim}}$ and $\Delta V_{h,\mathrm{dim}}$ are the radial and angular momentum direction components of the change in Dimorphos's velocity, respectively. We then assumed that the impulse on Dimorphos along $\hat{e}_{h,\mathrm{dim}}$, $\Delta V_{h,\mathrm{dim}}$, caused by the DART spacecraft is

$$\Delta V_{h,\mathrm{dim}} = \frac{m_{\mathrm{DART}}}{m_{\mathrm{dim}}}\vec{V}_\infty \cdot \hat{e}_{h,\mathrm{dim}} \tag{10}$$

with a conservative 100% 1σ uncertainty to account for the lack of information. The radial and along-track components were obtained from previous work (*15*).

Once we computed $\Delta\vec{V}_{\mathrm{dim}}$, we could project it along the Dimorphos surface normal direction at the impact site, $\hat{e}_{\mathrm{n,dim}}$. We used the latest digital terrain model of Dimorphos (*26*) to compute an averaged surface normal direction from a circular region with a radius of 1.5 m around the impact site. This was done because the nominal impact site on Dimorphos was situated between boulders (*38*), and we had to account for this in the computed value of $\hat{e}_{\mathrm{n,dim}}$. Using this value, we wrote the Dimorphos surface normal momentum enhancement factor, $\beta_{\mathrm{n,dim}}$, in a manner similar to Eq. 4 as

$$\beta_{\mathrm{n,dim}} = 1 + \frac{m_{\mathrm{dim}}\Delta V_{\mathrm{n,dim}} - m_{\mathrm{DART}}\vec{V}_\infty \cdot \hat{e}_{\mathrm{n,dim}}}{m_{\mathrm{DART}}\left[\left(\vec{V}_\infty \cdot \hat{e}_*\right)\hat{e}_* \cdot \hat{e}_{\mathrm{n,dim}}\right]} \tag{11}$$

where $\Delta V_{\mathrm{n,dim}} = \Delta\vec{V}_{\mathrm{dim}} \cdot \hat{e}_{\mathrm{n,dim}} = -2180 \pm 140\ \mu\mathrm{m\ s}^{-1}$ is the surface normal direction component of Dimorphos's velocity change due to DART. This yielded the reported value of $\beta_{\mathrm{n,dim}}$ in Table 1. Last, all the input parameters used in the above equations are listed in table S5.

Supplementary Materials

This PDF file includes:

Tables S1 to S5
References

REFERENCES

1. J. D. Carrillo-Sánchez, D. Nesvorná, P. Pokorná, D. Janches, J. M. C. Plane, Sources of cosmic dust in the Earth's atmosphere. *Geophys. Res. Lett.* **43**, 11979–11986 (2016).
2. A. W. Harris, P. W. Chodas, The population of near-earth asteroids revisited and updated. *Icarus* **365**, 114452 (2021).

3. L. W. Alvarez, Experimental evidence that an asteroid impact led to the extinction of many species 65 million years ago. *Proc. Natl. Acad. Sci. U.S.A.* **80**, 627–642 (1983).
4. O. P. Popova, P. Jenniskens, V. Emel'yanenko, A. Kartashova, E. Biryukov, S. Khaibrakhmanov, V. Shuvalov, Y. Rybnov, A. Dudorov, V. I. Grokhovsky, D. D. Badyukov, Q. Z. Yin, P. S. Gural, J. Albers, M. Granvik, L. G. Evers, J. Kuiper, V. Kharlamov, A. Solovyov, Y. S. Rusakov, S. Korotkiy, I. Serdyuk, A. V. Korochantsev, M. Y. Larionov, D. Glazachev, A. E. Mayer, G. Gisler, S. V. Gladkovsky, J. Wimpenny, M. E. Sanborn, A. Yamakawa, K. L. Verosub, D. J. Rowland, S. Roeske, N. W. Botto, J. M. Friedrich, M. E. Zolensky, L. le, D. Ross, K. Ziegler, T. Nakamura, I. Ahn, J. I. Lee, Q. Zhou, X. H. Li, Q. L. Li, Y. Liu, G. Q. Tang, T. Hiroi, D. Sears, I. A. Weinstein, A. S. Vokhmintsev, A. V. Ishchenko, P. Schmitt-Kopplin, N. Hertkorn, K. Nagao, M. K. Haba, M. Komatsu, T. Mikouchi, Chelyabinsk Airburst Consortium, Chelyabinsk airburst, damage assessment, meteorite recovery, and characterization. *Science* **342**, 1069–1073 (2013).
5. D. Nesvorný, R. Deienno, W. F. Bottke, R. Jedicke, S. Naidu, S. R. Chesley, P. W. Chodas, M. Granvik, D. Vokrouhlický, M. Brož, A. Morbidelli, E. Christensen, F. C. Shelly, B. T. Bolin, NEOMOD: A New Orbital Distribution Model for Near-Earth Objects. *Astron. J.* **166**, 55 (2023).
6. S. Larson, J. Brownlee, C. Hergenrother, T. Spahr, "The Catalina Sky Survey for NEOs," in *Bulletin of the American Astronomical Society* (American Astronomical Society, 1998), vol. 30, p. 1037.
7. N. Kaiser, H. Aussel, B. E. Burke, H. Boesgaard, K. Chambers, M. R. Chun, J. N. Heasley, K.-W. Hodapp, B. Hunt, R. Jedicke, D. Jewitt, R. Kudritzki, G. A. Luppino, M. Maberry, E. Magnier, D. G. Monet, P. M. Onaka, A. J. Pickles, Pui Hin H. Rhoads, T. Simon, A. Szalay, I. Szapudi, D. J. Tholen, J. L. Tonry, M. Waterson, J. Wick, "Pan-STARRS: A large synoptic survey telescope array," in *Survey and Other Telescope Technologies and Discoveries*, J. A. Tyson, S. Wolff, Eds. (SPIE, 2002); https://doi.org/10.1117/12.457365.
8. J. L. Tonry, An early warning system for asteroid impact. *Publ. Astron. Soc. Pac.* **123**, 58–73 (2011).
9. M. E. Schwamb, R. L. Jones, P. Yoachim, K. Volk, R. C. Dorsey, C. Opitom, S. Greenstreet, T. Lister, C. Snodgrass, B. T. Bolin, L. Inno, M. T. Bannister, S. Eggl, M. Solontoi, M. S. P. Kelley, M. Jurić, H. W. Lin, D. Ragozzine, P. H. Bernardinelli, S. R. Chesley, T. Daylan, J. Ďurech, W. C. Fraser, M. Granvik, M. M. Knight, C. M. Lisse, R. Malhotra, W. J. Oldroyd, A. Thirouin, Q. Ye, Tuning the Legacy Survey of Space and Time (LSST) observing strategy for solar system science. *Astrophys. J. Suppl. Ser.* **266**, 22 (2023).
10. A. K. Mainzer, J. R. Masiero, P. A. Abell, J. M. Bauer, W. Bottke, B. J. Buratti, S. J. Carey, D. Cotto-Figueroa, R. M. Cutri, D. Dahlen, P. R. M. Eisenhardt, Y. R. Fernandez, R. Furfaro, T. Grav, T. L. Hoffman, M. S. Kelley, Y. Kim, J. D. Kirkpatrick, C. R. Lawler, E. Lilly, X. Liu, F. Marocco, K. A. Marsh, F. J. Masci, C. W. McMurtry, M. Pourrahmani, L. Reinhart, M. E. Ressler, A. Satpathy, C. A. Schambeau, S. Sonnett, T. B. Spahr, J. A. Surace, M. Vaquero, E. L. Wright, G. R. Zengilowski, NEO Surveyor Mission Team, The Near-Earth Object Surveyor mission. *Planet. Sci. J.* **4**, 224 (2023).
11. J. Roa, D. Farnocchia, S. R. Chesley, A novel approach to asteroid impact monitoring. *Astron. J.* **162**, 277 (2021).
12. M. Fenucci, L. Faggioli, F. Gianotto, D. B. Cioci, J. L. Cano, L. Conversi, M. Devogèle, G. Di Girolamo, C. Drury, D. Föhring, L. Gisolfi, R. Kresken, M. Micheli, R. Moissl, F. Ocaña, D. Oliviero, A. Porru, P. Ramirez-Moreta, R. Rudawska, F. Bernardi, A. Bertolucci, L. Dimare, F. Guerra, V. Baldisserotto, M. Ceccaroni, R. Cennamo, A. Chessa, A. Del Vigna, D. Koschny, A. M. Teodorescu, E. Perozz, The Aegis orbit determination and impact monitoring system and services of the ESA NEOCC web portal. *Celest. Mech. Dyn. Astron.* **136**, 58 (2024).
13. N. L. Chabot, A. S. Rivkin, A. F. Cheng, O. S. Barnouin, E. G. Fahnestock, D. C. Richardson, A. M. Stickle, C. A. Thomas, C. M. Ernst, R. T. Daly, E. Dotto, A. Zinzi, S. R. Chesley, N. A. Moskovitz, B. W. Barbee, P. Abell, H. F. Agrusa, M. T. Bannister, J. Beccarelli, D. L. Bekker, M. B. Syal, B. J. Buratti, M. W. Busch, A. C. Bagatin, J. P. Chatelain, S. Chocron, G. S. Collins, L. Conversi, T. M. Davison, M. E. De Coster, J. D. P. Deshapriya, S. Eggl, R. C. Espiritu, T. L. Farnham, M. Ferrais, F. Ferrari, D. Föhring, O. Fuentes-Muñoz, I. Gai, C. Giordano, D. A. Glenar, E. Gomez, D. M. Graninger, S. F. Green, S. Greenstreet, P. H. Hasselmann, I. Herreros, M. Hirabayashi, M. Husárik, S. Ieva, S. L. Ivanovski, S. L. Jackson, E. Jehin, M. Jutzi, O. Karatekin, M. M. Knight, L. Kolokolova, K. M. Kumamoto, M. Küppers, F. L. Forgia, M. Lazzarin, J.-Y. Li, T. A. Lister, R. Lolachi, M. P. Lucas, A. Lucchetti, R. Luther, R. Makadia, E. M. Epifani, J. M. Mahon, G. Merisio, C. C. Merrill, A. J. Meyer, P. Michel, M. Micheli, A. Migliorini, K. Minker, D. Modenini, F. Moreno, N. Murdoch, B. Murphy, S. P. Naidu, H. Nair, R. Nakano, C. Opitom, J. Ormö, J. M. Owen, M. Pajola, E. E. Palmer, P. Palumbo, P. Panicucci, L. M. Parro, J. M. Pearl, A. Penttilä, D. Perna, E. Petrescu, P. Pravec, S. D. Raducan, K. T. Ramesh, R. Ridden-Harper, J. L. Rizos, A. Rossi, N. X. Roth, A. Rożek, B. Rozitis, E. V. Ryan, W. H. Ryan, P. Sánchez, T. Santana-Ros, D. J. Scheeres, P. Scheirich, C. B. Senel, C. Snodgrass, S. Soldini, D. Souami, T. S. Statler, R. Street, T. J. Stubbs, J. M. Sunshine, N. J. Tan, G. Tancredi, C. L. Tinsman, P. Tortora, F. Tusberti, J. D. Walker, C. D. Waller, K. Wünnemann, M. Zannoni, Y. Zhang, Achievement of the planetary defense investigations of the Double Asteroid Redirection Test (DART) mission. *Planet. Sci. J.* **5**, 49 (2024).
14. C. A. Thomas, S. P. Naidu, P. Scheirich, N. A. Moskovitz, P. Pravec, S. R. Chesley, A. S. Rivkin, D. J. Osip, T. A. Lister, L. A. M. Benner, M. Brozović, C. Contreras, N. Morrell, A. Rożek, P. Kušnirák, K. Hornoch, D. Mages, P. A. Taylor, A. D. Seymour, C. Snodgrass, U. G. Jørgensen, M. Dominik, B. Skiff, T. Polakis, M. M. Knight, T. L. Farnham, J. D. Giorgini, B. Rush, J. Bellerose, P. Salas, W. P. Armentrout, G. Watts, M. W. Busch, J. Chatelain, E. Gomez, S. Greenstreet, L. Phillips, M. Bonavita, M. J. Burgdorf, E. Khalouei, P. Longa-Peña, M. Rabus, S. Sajadian, N. L. Chabot, A. F. Cheng, W. H. Ryan, E. V. Ryan, C. E. Holt, H. F. Agrusa, Orbital period change of Dimorphos due to the DART kinetic impact. *Nature* **616**, 448–451 (2023).
15. S. P. Naidu, S. R. Chesley, N. Moskovitz, C. Thomas, A. J. Meyer, P. Pravec, P. Scheirich, D. Farnocchia, D. J. Scheeres, M. Brozovic, L. A. M. Benner, A. S. Rivkin, N. L. Chabot, Orbital and physical characterization of asteroid dimorphos following the DART impact. *Planet. Sci. J.* **5**, 74 (2024).
16. P. Scheirich, P. Pravec, A. J. Meyer, H. F. Agrusa, D. C. Richardson, S. R. Chesley, S. P. Naidu, C. Thomas, N. A. Moskovitz, Dimorphos orbit determination from mutual events photometry. *Planet. Sci. J.* **5**, 17 (2024).
17. T. J. Ahrens, A. W. Harris, Deflection and fragmentation of near-Earth asteroids. *Nature* **360**, 429–433 (1992).
18. J.-Y. Li, M. Hirabayashi, T. L. Farnham, J. M. Sunshine, M. M. Knight, G. Tancredi, F. Moreno, B. Murphy, C. Opitom, S. Chesley, D. J. Scheeres, C. A. Thomas, E. G. Fahnestock, A. F. Cheng, L. Dressel, C. M. Ernst, F. Ferrari, A. Fitzsimmons, S. Ieva, S. L. Ivanovski, T. Kareta, L. Kolokolova, T. Lister, S. D. Raducan, A. S. Rivkin, A. Rossi, S. Soldini, A. M. Stickle, A. Vick, J.-B. Vincent, H. A. Weaver, S. Bagnulo, M. T. Bannister, S. Cambioni, A. C. Bagatin, N. L. Chabot, G. Cremonese, R. T. Daly, E. Dotto, D. A. Glenar, M. Granvik, P. H. Hasselmann, I. Herreros, S. Jacobson, M. Jutzi, T. Kohout, F. L. Forgia, M. Lazzarin, Z.-Y. Lin, R. Lolachi, A. Lucchetti, R. Makadia, E. M. Epifani, P. Michel, A. Migliorini, N. A. Moskovitz, J. Ormö, M. Pajola, P. Sánchez, S. R. Schwartz, C. Snodgrass, J. Steckloff, T. J. Stubbs, J. M. Trigo-Rodríguez, Ejecta from the DART-produced active asteroid Dimorphos. *Nature* **616**, 452–456 (2023).
19. T. Kareta, C. Thomas, J. Y. Li, M. M. Knight, N. Moskovitz, A. Rożek, M. T. Bannister, S. Ieva, C. Snodgrass, P. Pravec, E. V. Ryan, W. H. Ryan, E. G. Fahnestock, A. S. Rivkin, N. Chabot, A. Fitzsimmons, D. Osip, T. Lister, G. Sarid, M. Hirabayashi, T. Farnham, G. Tancredi, P. Michel, R. Wainscoat, R. Weryk, B. Burrati, J. Pittichová, R. Ridden-Harper, N. J. Tan, P. Tristram, T. Brown, M. Bonavita, M. Burgdorf, E. Khalouei, P. Longa, M. Rabus, S. Sajadian, U. G. Jorgensen, M. Dominik, J. B. Kikwaya, E. Mazzotta Epifani, E. Dotto, P. Deshapriya, P. Hasselmann, M. Dall'Ora, L. Abe, T. Guillot, D. Mékarnia, A. Agabi, P. Bendjoya, O. Suarez, A. Triaud, T. Gasparetto, M. N. Günther, M. Kueppers, B. Merin, J. Chatelain, E. Gomez, H. Usher, C. Stoddard-Jones, M. Bartnik, M. Bellaver, B. Chetan, E. Dugan, T. Fallon, J. Fedewa, C. Gerhard, S. A. Jacobson, S. Painter, D. M. Peterson, J. E. Rodriguez, C. Smith, K. V. Sokolovsky, H. Sullivan, K. Townley, S. Watson, L. Webb, J. M. Trigo-Rodríguez, J. M. Llenas, I. Pérez-García, A. J. Castro-Tirado, J. B. Vincent, A. Migliorini, M. Lazzarin, L. Forgia, F. Ferrari, T. Polakis, B. Skiff, Ejecta evolution following a planned impact into an asteroid: The first five weeks. *Astrophys. J. Lett.* **959**, L12 (2023).
20. T. S. Statler, S. D. Raducan, O. S. Barnouin, M. E. De Coster, S. R. Chesley, B. Barbee, H. F. Agrusa, S. Cambioni, A. F. Cheng, E. Dotto, S. Eggl, E. G. Fahnestock, F. Ferrari, D. Graninger, A. Herique, I. Herreros, M. Hirabayashi, S. Ivanovski, M. Jutzi, Ö. Karatekin, A. Lucchetti, R. Luther, R. Makadia, F. Marzari, P. Michel, N. Murdoch, R. Nakano, J. Ormö, M. Pajola, A. S. Rivkin, A. Rossi, P. Sánchez, S. R. Schwartz, S. Soldini, D. Souami, A. Stickle, P. Tortora, J. M. Trigo-Rodríguez, F. Venditti, J.-B. Vincent, K. Wünnemann, After DART: Using the first full-scale test of a kinetic impactor to inform a future planetary defense mission. *Planet.Sci. J.* **3**, 244 (2022).
21. A. F. Cheng, H. F. Agrusa, B. W. Barbee, A. J. Meyer, T. L. Farnham, S. D. Raducan, D. C. Richardson, E. Dotto, A. Zinzi, V. D. Corte, T. S. Statler, S. Chesley, S. P. Naidu, M. Hirabayashi, J.-Y. Li, S. Eggl, O. S. Barnouin, N. L. Chabot, S. Chocron, G. S. Collins, R. T. Daly, T. M. Davison, M. E. De Coster, C. M. Ernst, F. Ferrari, D. M. Graninger, S. A. Jacobson, M. Jutzi, K. M. Kumamoto, R. Luther, J. R. Lyzhoft, P. Michel, N. Murdoch, R. Nakano, E. Palmer, A. S. Rivkin, D. J. Scheeres, A. M. Stickle, J. M. Sunshine, J. M. Trigo-Rodriguez, J.-B. Vincent, J. D. Walker, K. Wünnemann, Y. Zhang, M. Amoroso, I. Bertini, J. R. Brucato, A. Capannolo, G. Cremonese, M. Dall'Ora, P. J. D. Deshapriya, I. Gai, P. H. Hasselmann, S. Ieva, G. Impresario, S. L. Ivanovski, M. Lavagna, A. Lucchetti, E. M. Epifani, D. Modenini, M. Pajola, P. Palumbo, D. Perna, S. Pirrotta, G. Poggiali, A. Rossi, P. Tortora, M. Zannoni, G. Zanotti, Momentum transfer from the DART mission kinetic impact on asteroid Dimorphos. *Nature* **616**, 457–460 (2023).
22. R. Makadia, S. D. Raducan, E. G. Fahnestock, S. Eggl, Heliocentric effects of the DART mission on the (65803) Didymos binary asteroid system. *Planet. Sci. J.* **3**, 184 (2022).
23. R. Makadia, S. R. Chesley, D. Farnocchia, S. P. Naidu, D. Souami, P. Tanga, K. Tsiganis, M. Hirabayashi, S. Eggl, Measurability of the heliocentric momentum enhancement from a kinetic impact: The Double Asteroid Redirection Test (DART) mission. *Planet. Sci. J.* **5**, 38 (2024).
24. J. F. Ferreira, P. Tanga, F. Spoto, P. Machado, D. Herald, Asteroid astrometry by stellar occultations: Accuracy of the existing sample from orbital fitting. *Astron. Astrophys.* **658**, A73 (2022).
25. R. Makadia, D. Farnocchia, S. R. Chesley, S. Eggl, Gauss-Radau Small-body Simulator (GRSS): An open-source library for planetary defense. *Planet. Sci. J.* **6**, 85 (2025).

26. R. T. Daly, C. M. Ernst, O. S. Barnouin, R. W. Gaskell, H. Nair, H. Agrusa, N. L. Chabot, A. F. Cheng, E. Dotto, E. Mazzotta Epifani, R. C. Espiritu, T. L. Farnham, E. E. Palmer, P. Pravec, A. S. Rivkin, D. C. Waller, A. Zinzi, the DART and LICIACube teams, An updated shape model of Dimorphos from DART data. *Planet. Sci. J.* **5**, 24 (2024).
27. S. D. Raducan, M. Jutzi, A. F. Cheng, Y. Zhang, O. Barnouin, G. S. Collins, R. T. Daly, T. M. Davison, C. M. Ernst, T. L. Farnham, F. Ferrari, M. Hirabayashi, K. M. Kumamoto, P. Michel, N. Murdoch, R. Nakano, M. Pajola, A. Rossi, H. F. Agrusa, B. W. Barbee, M. B. Syal, N. L. Chabot, E. Dotto, E. G. Fahnestock, P. H. Hasselmann, I. Herreros, S. Ivanovski, J.-Y. Li, A. Lucchetti, R. Luther, J. Ormö, M. Owen, P. Pravec, A. S. Rivkin, C. Q. Robin, P. Sánchez, F. Tusberti, K. Wünnemann, A. Zinzi, E. M. Epifani, C. Manzoni, B. H. May, Physical properties of asteroid Dimorphos as derived from the DART impact. *Nat. Astron.* **8**, 445–455 (2024).
28. A. S. Rivkin, C. A. Thomas, I. Wong, B. Rozitis, J. de León, B. Holler, S. N. Milam, E. S. Howell, H. B. Hammel, A. Arredondo, J. R. Brucato, E. M. Epifani, S. Ieva, F. la Forgia, M. P. Lucas, A. Lucchetti, M. Pajola, G. Poggiali, J. N. Sunshine, J. M. Trigo-Rodríguez, Near to mid-infrared Spectroscopy of (65803) Didymos as observed by JWST: Characterization observations supporting the Double Asteroid Redirection Test. *Planet. Sci. J.* **4**, 214 (2023).
29. B. Carry, Density of asteroids. *Planet. Space Sci.* **73**, 98–118 (2012).
30. S. Abe, T. Mukai, N. Hirata, O. S. Barnouin-Jha, A. F. Cheng, H. Demura, R. W. Gaskell, T. Hashimoto, K. Hiraoka, T. Honda, T. Kubota, M. Matsuoka, T. Mizuno, R. Nakamura, D. J. Scheeres, M. Yoshikawa, Mass and local topography measurements of Itokawa by Hayabusa. *Science* **312**, 1344–1347 (2006).
31. S. C. Lowry, P. R. Weissman, S. R. Duddy, B. Rozitis, A. Fitzsimmons, S. F. Green, M. D. Hicks, C. Snodgrass, S. D. Wolters, S. R. Chesley, J. Pittichová, P. van Oers, The internal structure of asteroid (25143) Itokawa as revealed by detection of YORP spin-up. *Astron. Astrophys.* **562**, A48 (2014).
32. S. J. Ostro, J.-L. Margot, L. A. M. Benner, J. D. Giorgini, D. J. Scheeres, E. G. Fahnestock, S. B. Broschart, J. Bellerose, M. C. Nolan, C. Magri, P. Pravec, P. Scheirich, R. Rose, R. F. Jurgens, E. M. De Jong, S. Suzuki, Radar imaging of binary near-Earth asteroid (66391) 1999 KW4. *Science* **314**, 1276–1280 (2006).
33. H. F. Agrusa, Y. Zhang, D. C. Richardson, P. Pravec, M. Ćuk, P. Michel, R.-L. Ballouz, S. A. Jacobson, D. J. Scheeres, K. Walsh, O. Barnouin, R. T. Daly, E. Palmer, M. Pajola, A. Lucchetti, F. Tusberti, J. V. De Martini, F. Ferrari, A. J. Meyer, S. D. Raducan, P. Sánchez, Direct *N*-body simulations of satellite formation around small asteroids: Insights from DART's encounter with the Didymos system. *Planet. Sci. J.* **5**, 54 (2024).
34. O. Barnouin, R.-L. Ballouz, S. Marchi, J.-B. Vincent, H. Agrusa, Y. Zhang, C. M. Ernst, M. Pajola, F. Tusberti, A. Lucchetti, R. T. Daly, E. Palmer, K. J. Walsh, P. Michel, J. M. Sunshine, J. L. Rizos, T. L. Farnham, D. C. Richardson, L. M. Parro, N. Murdoch, C. Q. Robin, M. Hirabayashi, T. Kahout, E. Asphaug, S. D. Raducan, M. Jutzi, F. Ferrari, P. H. A. Hasselmann, A. C. Bagatin, N. L. Chabot, J.-Y. Li, A. F. Cheng, M. C. Nolan, A. M. Stickle, O. Karatekin, E. Dotto, V. D. Corte, E. M. Epifani, A. Rossi, I. Gai, J. D. P. Deshapriya, I. Bertini, A. Zinzi, J. M. Trigo-Rodriguez, J. Beccarelli, S. L. Ivanovski, J. R. Brucato, G. Poggiali, G. Zanotti, M. Amoroso, A. Capannolo, G. Cremonese, M. Dall'Ora, S. Ieva, G. Impresario, M. Lavagn, D. Modenini, P. Palumbo, D. Perna, S. Pirrotta, P. Tortora, M. Zannoni, A. S. Rivkin, The geology and evolution of the near-Earth binary asteroid system (65803) Didymos. *Nat. Commun.* **15**, 6202 (2024).
35. M. Pajola, F. Tusberti, A. Lucchetti, O. Barnouin, S. Cambioni, C. M. Ernst, E. Dotto, R. T. Daly, G. Poggiali, M. Hirabayashi, R. Nakano, E. M. Epifani, N. L. Chabot, V. D. Corte, A. Rivkin, H. Agrusa, Y. Zhang, L. Penasa, R.-L. Ballouz, S. Ivanovski, N. Murdoch, A. Rossi, C. Robin, S. Ieva, J. B. Vincent, F. Ferrari, S. D. Raducan, A. Campo-Bagatin, L. Parro, P. Benavidez, G. Tancredi, Ö. Karatekin, J. M. Trigo-Rodriguez, J. Sunshine, T. Farnham, E. Asphaug, J. D. P. Deshapriya, P. H. A. Hasselmann, J. Beccarelli, S. R. Schwartz, P. Abell, P. Michel, A. Cheng, J. R. Brucato, A. Zinzi, M. Amoroso, S. Pirrotta, G. Impresario, I. Bertini, A. Capannolo, S. Caporali, M. Ceresoli, G. Cremonese, M. Dall'Ora, I. Gai, L. G. Casajus, E. Gramigna, R. L. Manghi, M. Lavagna, M. Lombardo, D. Modenini, P. Palumbo, D. Perna, P. Tortora, M. Zannoni, G. Zanotti, Evidence for multi-fragmentation and mass shedding of boulders on rubble-pile binary asteroid system (65803) Didymos. *Nat. Commun.* **15**, 6205 (2024).
36. J.-L. Margot, P. Pravec, P. Taylor, B. Carry, S. Jacobson, "Asteroid systems: Binaries, triples, and pairs," in *Asteroids IV*, W. F. Bottke, F. E. DeMeo, P. Michel, Eds. (University of Arizona Press, 2015), p. 373.
37. M. Hirabayashi, S. D. Raducan, J. M. Sunshine, T. L. Farnham, J. D. P. Deshapriya, J.-Y. Li, G. Tancredi, S. R. Chesley, R. T. Daly, C. M. Ernst, I. Gai, P. H. Hasselmann, S. P. Naidu, H. Nair, E. E. Palmer, C. D. Waller, A. Zinzi, H. F. Agrusa, B. W. Barbee, M. B. Syal, G. S. Collins, T. M. Davison, M. E. De Coster, M. Jutzi, K. M. Kumamoto, N. A. Moskovitz, J. R. Lyzhoft, S. R. Schwartz, P. A. Abell, O. S. Barnouin, N. L. Chabot, A. F. Cheng, E. Dotto, E. G. Fahnestock, P. Michel, D. C. Richardson, A. S. Rivkin, A. M. Stickle, C. A. Thomas, J. Beccarelli, J. R. Brucato, M. Dall'Ora, V. D. Corte, E. M. Epifani, S. Ieva, G. Impresario, S. Ivanovski, A. Lucchetti, D. Modenini, M. Pajola, P. Palumbo, S. Pirrotta, G. Poggiali, A. Rossi, P. Tortora, F. Tusberti, M. Zannoni, G. Zanotti, F. Ferrari, D. A. Glenar, I. Herreros, S. A. Jacobson, Ö. Karatekin, M. Lazzarin, R. Lolachi, M. P. Lucas, R. Makadia, F. Marzari, C. C. Merrill, A. Migliorini, R. Nakano, J. Ormö, P. Sánchez, C. B. Senel, S. Soldini, T. J. Stubbs, Elliptical ejecta of asteroid Dimorphos is due to its surface curvature. *Nat. Commun.* **16**, 1602 (2025).
38. R. T. Daly, C. M. Ernst, O. S. Barnouin, N. L. Chabot, A. S. Rivkin, A. F. Cheng, E. Y. Adams, H. F. Agrusa, E. D. Abel, A. L. Alford, E. I. Asphaug, J. A. Atchison, A. R. Badger, P. Baki, R.-L. Ballouz, D. L. Bekker, J. Bellerose, S. Bhaskaran, B. J. Buratti, S. Cambioni, M. H. Chen, S. R. Chesley, G. Chiu, G. S. Collins, M. W. Cox, M. E. De Coster, P. S. Ericksen, R. C. Espiritu, A. S. Faber, T. L. Farnham, F. Ferrari, Z. J. Fletcher, R. W. Gaskell, D. M. Graninger, M. A. Haque, P. A. Harrington-Duff, S. Hefter, I. Herreros, M. Hirabayashi, P. M. Huang, S.-Y. W. Hsieh, S. A. Jacobson, S. N. Jenkins, M. A. Jensenius, J. W. John, M. Jutzi, T. Kohout, T. O. Krueger, F. E. Laipert, N. R. Lopez, R. Luther, A. Lucchetti, D. M. Mages, S. Marchi, A. C. Martin, M. E. McQuaide, P. Michel, N. A. Moskovitz, I. W. Murphy, N. Murdoch, S. P. Naidu, H. Nair, M. C. Nolan, J. Ormö, M. Pajola, E. E. Palmer, J. M. Peachey, P. Pravec, S. D. Raducan, K. T. Ramesh, J. R. Ramirez, E. L. Reynolds, J. E. Richman, C. Q. Robin, L. M. Rodriguez, L. M. Roufberg, B. P. Rush, C. A. Sawyer, D. J. Scheeres, P. Scheirich, S. R. Schwartz, M. P. Shannon, B. N. Shapiro, C. E. Shearer, E. J. Smith, R. J. Steele, J. K. Steckloff, A. M. Stickle, J. M. Sunshine, E. A. Superfin, Z. B. Tarzi, C. A. Thomas, J. R. Thomas, J. M. Trigo-Rodríguez, B. T. Tropf, A. T. Vaughan, D. Velez, C. D. Waller, D. S. Wilson, K. A. Wortman, Y. Zhang, Successful kinetic impact into an asteroid for planetary defence. *Nature* **616**, 443–447 (2023).
39. P. Michel, M. Küppers, A. C. Bagatin, B. Carry, S. Charnoz, J. de Leon, A. Fitzsimmons, P. Gordo, S. F. Green, A. Hérique, M. Juzi, Ö. Karatekin, T. Kohout, M. Lazzarin, N. Murdoch, T. Okada, E. Palomba, P. Pravec, C. Snodgrass, P. Tortora, K. Tsiganis, S. Ulamec, J.-B. Vincent, K. Wünnemann, Y. Zhang, S. D. Raducan, E. Dotto, N. Chabot, A. F. Cheng, A. Rivkin, O. Barnouin, C. Ernst, A. Stickle, D. C. Richardson, C. Thomas, M. Arakawa, H. Miyamoto, A. Nakamura, S. Sugita, M. Yoshikawa, P. Abell, E. Asphaug, R.-L. Ballouz, W. F. Bottke Jr., D. S. Lauretta, K. J. Walsh, P. Martino, I. Carnelli, The ESA Hera mission: Detailed characterization of the DART impact outcome and of the binary asteroid (65803) Didymos. *Planet. Sci. J.* **3**, 160 (2022).
40. D. Farnocchia, S. R. Chesley, Y. Takahashi, B. Rozitis, D. Vokrouhlický, B. P. Rush, N. Mastrodemos, B. M. Kennedy, R. S. Park, J. Bellerose, D. P. Lubey, D. Velez, A. B. Davis, J. P. Emery, J. M. Leonard, J. Geeraert, P. G. Antreasian, D. S. Lauretta, Ephemeris and hazard assessment for near-Earth asteroid (101955) Bennu based on OSIRIS-REx data. *Icarus* **369**, 114594 (2021).
41. A. Milani, G. Gronchi, *Theory of Orbit Determination* (Cambridge University Press, 2009).
42. M. Carpino, A. Milani, S. R. Chesley, Error statistics of asteroid optical astrometric observations. *Icarus* **166**, 248–270 (2003).
43. D. Farnocchia, S. R. Chesley, D. Vokrouhlicky, A. Milani, F. Spoto, Near Earth asteroids with measurable Yarkovsky effect. *Icarus* **224**, 1–13 (2013).
44. D. Farnocchia, S. R. Chesley, D. J. Tholen, M. Micheli, High precision predictions for near-Earth asteroids: The strange case of (3908) Nyx. *Celest. Mech. Dyn. Astron.* **119**, 301–312 (2014).
45. G. J. Bierman, *Factorization Methods For Discrete Sequential Estimation* (Academic Press, 1977).
46. J. D. Feldhacker, M. B. Syal, B. A. Jones, A. Doostan, J. M. Mahon, D. J. Scheeres, Shape dependence of the kinetic deflection of asteroids. *J. Guid. Control Dynam.* **40**, 2417–2431 (2017).
47. A. M. Stickle, M. E. De Coster, C. Burger, W. K. Caldwell, D. Graninger, K. M. Kumamoto, R. Luther, J. Ormö, S. Raducan, E. Rainey, C. M. Schäfer, J. D. Walker, Y. Zhang, P. Michel, J. M. Owen, O. Barnouin, A. F. Cheng, S. Chocron, G. S. Collins, T. M. Davison, E. Dotto, F. Ferrari, M. I. Herreros, S. L. Ivanovski, M. Jutzi, A. Lucchetti, E. Martellato, M. Pajola, C. S. Plesko, M. B. Syal, S. R. Schwartz, J. M. Sunshine, K. Wünnemann, Effects of impact and target parameters on the results of a kinetic impactor: Predictions for the Double Asteroid Redirection Test (DART) mission. *Planet. Sci. J.* **3**, 248 (2022).
48. J. D. Giorgini, D. K. Yeomans, A. B. Chamberlin, P. W. Chodas, R. A. Jacobson, M. S. Keesey, J. H. Lieske, S. J. Ostro, E. M. Standish, R. N. Wimberly, "JPL's on-line solar system data service," in *AAS/Division for Planetary Sciences Meeting Abstracts* (American Astronomical Society, 1996), vol. 28, p. 1158.

Acknowledgments: This research used data and services provided by the International Astronomical Union Minor Planet Center. We would like to acknowledge the observers and measurers involved in the Didymos occultation campaigns: A. Asai, E. Barbotin, J. Broughton, N. Carlson, A. Cazaux, S. Cikota, K. Cobble, F. Colas, J. Dauvergne, R. Dunford, D. Dunham, J. Dunham, J. Flores, D. Gault, K. Getrost, K. Guhl, J. Hanus, T. Hayamizu, D. Herald, K. Hosoi, M. Ida, R. Jones, K. Kitazaki, G. Langin, A. Leroy, B. Lott, G. Lyzenga, P. Maley, N. Manago, A. Manna, J. Moore, Y. Nakamura, T. Nemoto, H. Noda, R. Nolthenius, S. Preston, L. Rousselot, M. Sanchez, M. Skrutskie, S. Sposetti, M. Takimoto, R. Trank, R. Venable, H. Watanabe, F. Weber, B. Whitehurst, H. Yamamura, M. Yamashita, and H. Yoshihara. The results shown here were directly enabled by these not-so-amateur astronomers' efforts to go out into the middle of nowhere and observe the necessary stellar occultations. **Funding:** R.M. acknowledges funding from a NASA Space Technology Graduate Research Opportunities (NSTGRO) award, NASA contract no. 80NSSC22K1173. The work of S.R.C., D.F., and S.P.N. was carried out at the Jet Propulsion Laboratory, California Institute of Technology, under a contract with the National Aeronautics

and Space Administration (no. 80NM0018D0004). The ACROSS occultation collaboration, which coordinated many of the stellar occultation measurements, was supported under the OSIP ESA contract no. 4000135299/21/NL/GLC/ov by the Programme Nationale de Planétologie and by the BQR program of Observatoire de la Côte d'Azur. **Author contributions:** R.M.: Writing—original draft, conceptualization, investigation, writing—review and editing, methodology, resources, funding acquisition, data curation, validation, supervision, formal analysis, software, project administration, and visualization. S.R.C.: Conceptualization, investigation, writing—review and editing, methodology, validation, supervision, formal analysis, software, and visualization. D.H.: Investigation, methodology, and formal analysis. D.F.: Conceptualization, writing—review and editing, and methodology. S.P.N.: Conceptualization, investigation, and writing—review and editing. N.L.C.: Writing—review and editing, funding acquisition, and project administration. A.S.R.: Conceptualization, writing—review and editing, and resources. A.S.: Investigation, writing—review and editing, data curation, and validation. D.S.: Investigation, writing—review and editing, resources, and formal analysis. P.T.: Conceptualization, investigation, writing—review and editing, methodology, data curation, validation, software, and project administration. S.T.: Investigation, writing—review and editing, and data curation. K.T.: Conceptualization, investigation, writing—review and editing, data curation, and validation. S.B.: Investigation, validation, formal analysis, and software. S.E.: Conceptualization, writing—review and editing, methodology, resources, funding acquisition, validation, supervision, software, and project administration. **Competing interests:** The authors declare that they have no competing interests. **Data, code, and materials availability:** The publicly available Gauss-Radau Small-body Simulator (GRSS) library (https://pypi.org/project/grss) was used to perform the analysis presented here. The Didymos optical astrometry is available to the public via the International Astronomical Union Minor Planet Center (www.minorplanetcenter.net/db_search/show_object?utf8=), and the radar astrometry is publicly available from the Solar System Dynamics Group at the Jet Propulsion Laboratory (https://ssd.jpl.nasa.gov/tools/sbdb_lookup.html#/?sstr=65803&view=OPR). All data and code needed to evaluate and reproduce the results in the paper are present in the paper and/or the Supplementary Materials.

Submitted 13 July 2025
Accepted 29 January 2026
Published 6 March 2026
10.1126/sciadv.aea4259

ScienceAdvances

Direct detection of an asteroid's heliocentric deflection: The Didymos system after DART

Rahil Makadia, Steven R. Chesley, David Herald, Davide Farnocchia, Nancy L. Chabot, Shantanu P. Naidu, Andrew S. Rivkin, Alexandros Siakas, Damya Souami, Paolo Tanga, Sotirios Tsavdaridis, Kleomenis Tsiganis, Sébastien Bouquillon, and Siegfried Eggl

Sci. Adv. **12** (10), eaea4259. DOI: 10.1126/sciadv.aea4259